Measurement 200 (2022) 111618

Contents lists available at ScienceDirect

Measurement

journal homepage: www.elsevier.com/locate/measurement

General line-line method for propagation constant measurement of non-reciprocal networks

Ugur Cem Hasar [a,*], Hamdullah Ozturk [a], Huseyin Korkmaz [a], Mucahit Izginli [a,b], Muharrem Karaaslan [c], Musa Bute [a]

[a] *Department of Electrical and Electronics Engineering, Gaziantep University, 27310 Gaziantep, Turkey*
[b] *Department of Electrical and Electronics Engineering, Hasan Kalyoncu University, 27410 Gaziantep, Turkey*
[c] *Department of Electrical and Electronics Engineering, Iskenderun Technical University, 31200 Iskenderun, Hatay, Turkey*

ARTICLE INFO

Keywords:
Line-line method
Nonreciprocal network
Propagation constant

ABSTRACT

A general "line-line" (LL) method is proposed for propagation constant determination (γ^+ and γ^-) of nonreciprocal networks using multiple reference networks. The new formalism provides flexibility in implementation of LL methods so that not only more accurate γ^+ (and γ^-) could be retrieved but also the effect of inaccurate length information of the non-reciprocal network on γ^+ (and γ^-) evaluation could be suppressed. For validation of the method, γ^+ and γ^- of a microwave phase shifter (a nonreciprocal network) are determined using uncalibrated scattering parameter measurements at X-band (8.2–12.4 GHz). Two different statistical analyses based on normalized root-mean-square-error and goodness of fit and based on coefficient of variation and confidence interval are individually performed to evaluate the performance and accuracy of our method.

1. Introduction

Propagation constant or electromagnetic properties of materials/networks can be determined from uncalibrated or raw scattering (S-) parameters using the "line-line" (LL) methods [1–5]. LL methods use various forms of guiding structures such as coaxial transmission line [1], microstrip line [2], slotline [3], rectangular waveguide [4], and coplanar waveguide [5] for such determination. The LL methods in the literature can be categorized into (a) two identical lines with different lengths loaded by the same material [2,6,3,7–9], (b) two identical lines with the same length loaded by different materials [1,4,10], and (c) non-zero length and zero-length lines loaded with the same/different materials [5,11–15]. When these methods are examined, it is noticed that the reference network is limited with propagation constant, impedance, or length. In our recent study, we have proposed an improved LL method using a reference network with arbitrary forward and backward impedance, propagation constant, and length, thus giving flexibility in the application of LL methods [16]. Nonetheless, all these LL methods [2,6,3,7–9,5,11–16] are restricted to reciprocal networks assuming the same forward and backward propagation constants.

In recent studies, we proposed two LL methods applicable for reciprocal and non-reciprocal networks [17,18]. Such an analysis could be utilized for examining propagation characteristics of microwave phase shifter networks [18,17] or chiral materials [19,20]. There is a main disadvantage of these methods [17,18]. They assume that reciprocal (or non-reciprocal) lines have the same electromagnetic properties (the same forward (and backward) propagation constants and the same wave impedances) but different lengths. In some applications, it is difficult to have two reciprocal lines having identical properties with different lengths. Using a zero-length non-reciprocal line (the thru connection) could be a remedy for such circumstances. However, as to be demonstrated in Section 3, using a zero-length line could increase the measured uncertainty in determination of forward (and backward) propagation constant of non-reciprocal lines. Besides, it will also be shown by measurements in Section 3 that any small deviation from the actual value of the non-reciprocal line may affect seriously the evaluation of its forward (and backward) propagation constant if the thru connection is utilized in measurements.

In the submitted work, we extend the studies [17,18] and propose a more general LL method applicable for forward/backward propagation constant measurement of non-reciprocal (or reciprocal) reflecting (or non-reflecting) networks using a reference network with arbitrary propagation constant(s), impedance, and length. A statistical analysis based on normalized root-mean-square-error (N-RMSE) and goodness of fit (GoF) and another statistical analysis based on coefficient of variation (COV) and confidence interval (CI) are individually performed to evaluate the performance and accuracy of our method. In addition to

* Corresponding author.
E-mail address: uchasar@gantep.edu.tr (U.C. Hasar).

https://doi.org/10.1016/j.measurement.2022.111618
Received 25 April 2022; Received in revised form 2 July 2022; Accepted 8 July 2022
Available online 22 July 2022

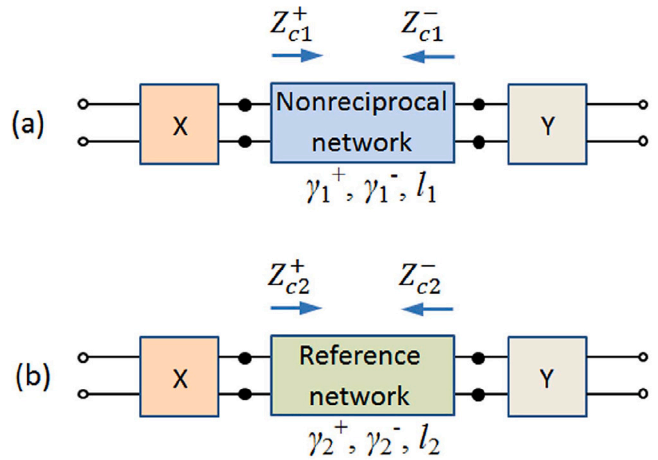

Fig. 1. Two configurations for the application of general LL method: (a) Nonreciprocal network and (b) reference network.

its advantage of allowing lines with different lengths loaded by various materials, it will be demonstrated by measurements that the proposed formalism has the capability of improving the measurement accuracy (reducing the uncertainties) and can reduce the effect of inaccurate length information of non-reciprocal line/networks.

2. The generalized LL method

2.1. Formalism

Figs. 1(a) and 1(b) illustrate the measurement configurations of a nonreciprocal network and a reference network for implementation of the proposed general LL method for determination of the forward and backward propagation constants γ_1^+ and γ_1^- of this nonreciprocal network with forward and backward wave impedances Z_{c1}^+ and Z_{c1}^-, and the length l_1. To make the analysis general, the reference network is also assumed to be nonreciprocal with the forward and backward propagation constants γ_2^+ and γ_2^-, forward and backward wave impedances Z_{c2}^+ and Z_{c2}^-, and the length l_2. Here, the reference network refers to a network (with known γ_2^+, γ_2^-, Z_{c2}^+, Z_{c2}^-, and l_2) used to determine γ_1^+ and γ_1^- without any knowledge of error networks, to be discussed shortly. The overall wave-cascading matrix (WCM) presentations of the configurations in Figs. 1(a) and 1(b) are

$$M_1 = X \cdot R_1^{Z_0,Z_0}(l_1) \cdot Y, \tag{1}$$

$$M_2 = X \cdot R_2^{Z_0,Z_0}(l_2) \cdot Y, \tag{2}$$

where M_1 and M_2 denote, respectively, the overall WCMs of the nonreciprocal and reference networks in Figs. 1(a) and 1(b); X and Y denote the WCMs of error networks involving tracking (frequency) errors, source and load match errors, and hardware imperfection of the vector network analyzer (VNA); $R_1^{Z_0,Z_0}(l_1)$ and $R_2^{Z_0,Z_0}(l_2)$ represent the WCMs of the nonreciprocal and reference networks referenced to the same characteristic impedance Z_0, involving impedance transformation from Z_0 to Z_{c1}^+ and Z_{c2}^+, amplitude and phase variations along the lines with l_1 and l_2, and impedance transformation from Z_{c1}^+ and Z_{c2}^+ to Z_0, respectively. For this reason, Z_0 appears two times in the superscripts of $R_1^{Z_0,Z_0}(l_1)$ and $R_2^{Z_0,Z_0}(l_2)$ networks. It is assumed that the error networks X and Y do not change for both configurations in Figs. 1(a) and 1(b).

The WCM $R_1^{Z_0,Z_0}(l_1)$ can be decomposed into [21,22]

$$R_1^{Z_0,Z_0}(l_1) = Q^{Z_0,Z_{c1}^\pm} \cdot R_1^{Z_{c1}^\pm,Z_{c1}^\pm}(l_1) \cdot Q^{Z_{c1}^\pm,Z_0}, \tag{3}$$

$$R_2^{Z_0,Z_0}(l_2) = Q^{Z_0,Z_{c2}^\pm} \cdot R_2^{Z_{c2}^\pm,Z_{c2}^\pm}(l_2) \cdot Q^{Z_{c2}^\pm,Z_0}, \tag{4}$$

where $Q^{Z_0,Z_{c1}^\pm}$, $Q^{Z_{c1}^\pm,Z_0}$, $Q^{Z_0,Z_{c2}^\pm}$, and $Q^{Z_{c2}^\pm,Z_0}$ are the impedance transformation WCMs which are functions of Z_{c1}^+, Z_{c1}^-, Z_{c2}^+, and Z_{c2}^- defined for $u = 1$ and 2 by [16]

$$Q^{Z_0,Z_{cu}^\mp} = \kappa_u \begin{bmatrix} 1 & \Gamma_u^+ \\ \Gamma_u^- & 1 \end{bmatrix}, \quad Q^{Z_{cu}^\mp,Z_0} = \left(Q^{Z_0,Z_{cu}^\mp}\right)^{-1}, \tag{5}$$

$$\Gamma_u^+ = \frac{Z_{cu}^+ - Z_0}{Z_{cu}^+ + Z_0}, \quad \Gamma_u^- = \frac{Z_{cu}^- - Z_0}{Z_{cu}^- + Z_0}. \tag{6}$$

Here, Γ_u^+ and Γ_u^- are, respectively, the reflection coefficients due to impedance transformations from Z_0 to Z_{cu}^+ and from Z_0 to Z_{cu}^-. Besides, $R_1^{Z_{c1}^\pm,Z_{c1}^\pm}(l_1)$ and $R_2^{Z_{c2}^\pm,Z_{c2}^\pm}(l_2)$ can be expressed [18,17]

$$R_u^{Z_{cu}^\pm,Z_{cu}^\pm}(l_u) = \begin{bmatrix} T_u^- & 0 \\ 0 & 1/T_u^+ \end{bmatrix}, \quad T_u^\mp = e^{-\gamma_u^\mp l_u}. \tag{7}$$

It is obvious from (1) and (2) that the effect of X and Y must be eliminated to characterize the nonreciprocal network. From (1) and (2), one can determine

$$M_1 M_2^{-1} = X \cdot R_1^{Z_0,Z_0}(l_1) \cdot [R_2^{Z_0,Z_0}(l_2)]^{-1} \cdot X^{-1}, \tag{8}$$

where '$\star^{-1}$' is the inverse of the square matrix $\star$. It is seen from (8) that the effect of Y is already eliminated.

Using the decompositions in (3) and (4), the product $R_1^{Z_0,Z_0}(l_1) \cdot [R_2^{Z_0,Z_0}(l_2)]^{-1}$ can be re-written as

$$\begin{aligned} R_1^{Z_0,Z_0}(l_1) \cdot [R_2^{Z_0,Z_0}(l_2)]^{-1} &= Q^{Z_0,Z_{c1}^\pm} \cdot R_1^{Z_{c1}^\pm,Z_{c1}^\pm}(l_1) \\ &\cdot Q^{Z_{c1}^\pm,Z_{c2}^\pm} \cdot [R_2^{Z_{c2}^\pm,Z_{c2}^\pm}(l_2)]^{-1} \cdot Q^{Z_{c2}^\pm,Z_{c1}^\pm} \cdot (Q^{Z_0,Z_{c1}^\pm})^{-1}. \end{aligned} \tag{9}$$

On the other hand, by taking the trace operation of $M_1 M_2^{-1}$, which is the sum of eigenvalues of $M_1 M_2^{-1}$, we determine

$$\begin{aligned} \mathrm{Tr}(M_1 M_2^{-1}) = \Lambda_1 = \mathrm{Tr}\Big(& R_1^{Z_{c1}^\pm,Z_{c1}^\pm}(l_1) \cdot Q^{Z_{c1}^\pm,Z_{c2}^\pm} \\ & \cdot [R_2^{Z_{c2}^\pm,Z_{c2}^\pm}(l_2)]^{-1} \cdot Q^{Z_{c2}^\pm,Z_{c1}^\pm} \Big), \end{aligned} \tag{10}$$

where Tr($\star$) denotes the trace of '$\star$'. Here, the effect of X (in addition to $Q^{Z_0,Z_{c1}^\pm}$) is eliminated due to trace invariant property with respect to a change of basis.

After some manipulations, one can derive

$$\Lambda_1 = \frac{T_1^+ T_1^- + T_2^+ T_2^- - (1 + T_1^+ T_1^- T_2^+ T_2^-)\Gamma_\delta}{T_1^+ T_2^- (1 - \Gamma_\delta)}, \tag{11}$$

where

$$\Gamma_\delta = 1 - \frac{\left(1 - \Gamma_1^+ \Gamma_1^-\right)\left(1 - \Gamma_2^+ \Gamma_2^-\right)}{\left(1 - \Gamma_1^+ \Gamma_2^-\right)\left(1 - \Gamma_1^- \Gamma_2^+\right)}. \tag{12}$$

Furthermore, following (3)–(10), it is possible to obtain

$$\Lambda_2 = \frac{T_1^+ T_1^- + T_2^+ T_2^- - (1 + T_1^+ T_1^- T_2^+ T_2^-)\Gamma_\delta}{T_1^- T_2^+ (1 - \Gamma_\delta)}, \tag{13}$$

where $\Lambda_2 = \mathrm{Tr}(M_2 M_1^{-1})$. From (11) and (13), T_1^- can be expressed by T_1^+ as

$$T_1^- = \left(\Lambda_1/\Lambda_2\right)\left(T_2^-/T_2^+\right) T_1^+. \tag{14}$$

2.2. Validation

If nonreciprocal and reference networks are reciprocal and have different lengths ($l_1 \neq l_2$) but the same symmetric reflection, $\gamma_1^+ = \gamma_1^- = \gamma_1$, $\gamma_2^+ = \gamma_2^- = \gamma_2$, and $Z_{c1}^+ = Z_{c1}^- = Z_{c1} = Z_{c2}^+ = Z_{c2}^- = Z_{c2} = Z_c$. Then, (11) (or (13)) reduces to a form similar in the studies [6]. Furthermore, if the nonreciprocal network is assumed to be reciprocal with symmetric/asymmetric reflections and the reference network has

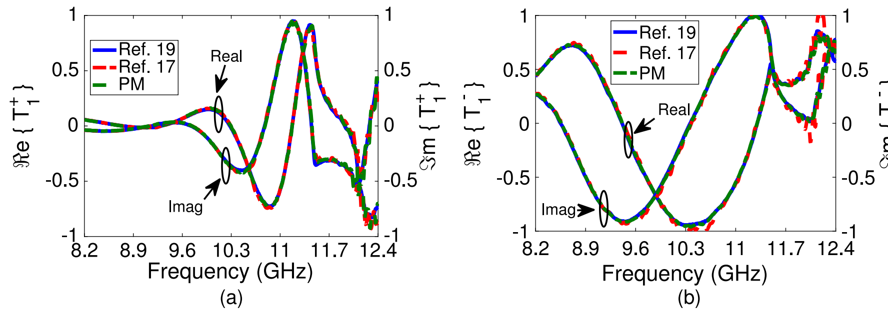

Fig. 2. Extracted real and imaginary parts of (a) T_1^+ and (b) T_1^- of the microwave phase shifter by the method in [19] (denoted by Ref. [19]), the calibration-independent method [18] (denoted by Ref. [18]), and the proposed method (denoted by PM).

$l_2 = 0$ (thru connection), then (11) (or (13)) reduces to a form similar in the study [12]. Finally, if the reference network (nonreciprocal) has $l_2 = 0$ ($T_2^+ = T_2^- = 1$), then (11) reduces to a form similar to (23) in the study [18]:

$$\Lambda_1 = 1/T_1^+ + T_1^-, \tag{15}$$

and then it is possible to evaluate T^+ and T^- following the procedure in [18]. All the above cases validate our proposed formalism in (11) and (13).

2.3. Implementation and accuracy improvement

Although $l_2 = 0$ in (11) facilitates the evaluation of T_1^+ and T_1^- in a simple manner using the procedure [18], the accuracy of such a procedure, as will be shown in Section 3, has a limited accuracy. To improve the accuracy of T_1^+ and T_1^- determination, we consider application of multiple reference networks. For simplicity and from a practical point of view, it is assumed that the reference network is reciprocal. Then, using two identical reciprocal reference networks with lengths l_2 and l_3, one can derive the objective function for T_1^+ using (11) and (13)

$$\begin{aligned} F_{\rm obj}(T_1^+) &= \left(\Lambda_1/\Lambda_2\right)\left(\Lambda_3/\Lambda_4\right)\left(T_3^2 - T_2^2\right)(T_1^+)^4 \\ &+ \Lambda_1\Lambda_3\left[T_3\left(T_2^2-1\right)/\Lambda_2 - T_2\left(T_3^2-1\right)/\Lambda_4\right](T_1^+)^3 \\ &+ \left(\Lambda_1/\Lambda_2 - \Lambda_3/\Lambda_4\right)(1 - T_2^2T_3^2)(T_1^+)^2 \\ &+ \left[(\Lambda_3T_3 - \Lambda_1T_2) + (\Lambda_1T_3 - \Lambda_3T_2)T_2T_3\right]T_1^+ \\ &+ (T_2^2 - T_3^2) = 0. \end{aligned} \tag{16}$$

where $T_2^{\mp} = e^{-\gamma_2^{\mp}l_2} = T_2$, $T_3^{\mp} = e^{-\gamma_2^{\mp}l_3} = T_3$, $\Lambda_3 = \mathrm{Tr}(M_2M_3^{-1})$, $\Lambda_4 = \mathrm{Tr}(M_2^{-1}M_3)$, and M_3 denotes the WCM of the reference network with length l_3. The correct root for T_1^+ can be evaluated from (16) by using the 'roots' function of MATLAB© and enforcing the passivity principle ($|T_1^+| \le 1$) where $|\star|$ denotes the magnitude of '$\star$'.

Once T_1^+ is computed from (16), T_1^- can be evaluated from (14). Finally, γ_1^+ and γ_1^- can be determined from

$$\gamma_1^{\mp} = \alpha_1^{\mp} + j\beta_1^{\mp} = \frac{-\ln(T_1^{\mp}) + j2\pi m_b^{\mp}}{l_1}, \tag{17}$$

where α_1^+, α_1^-, β_1^+, and β_1^- are, respectively, the forward and backward attenuation and phase constants; and m_b^+ and m_b^- are the branch indices with values of $0, \mp1, \mp2 \ldots$. Their correct values can be ascertained by the stepwise technique [23] or the phase unwrapping method [24].

3. Measurements and discussion

3.1. Experimental setup and validation of the method

A rectangular waveguide measurement setup operating at X-band (8.2–12.4 GHz) was constructed for validation of the proposed general LL method for reciprocal networks [17,18]. It has a handheld vector network analyzer VNA (N9918A) from Keysight Technologies, two rugged coaxial cables, and two longer waveguide straights. In implementation of our method, two empty waveguide straights with lengths l_2 = 7.70 mm and l_3 = 9.40 mm were considered as reference networks. As for the nonreciprocal network, a microwave phase shifter with length l_1 = 28.7 mm was used. For all S-parameter measurements by our method, the measurement setup was not calibrated by any calibration technique. The method [19] and the method [18] were also applied to extract T_1^+, T_1^-, γ_1^+, and γ_1^- quantities of this shifter. In application of the method [18], uncalibrated S-parameters of the shifter and the thru-connection were used. On the other hand, in the application of the method [19], calibrated S-parameters of the shifter were measured. For the calibration of the measurement setup, the TRL calibration technique was employed. A highly reflective short was utilized as a reflect standard and a 9.40 mm empty waveguide section was implemented as the line standard which produced $\mp$70° phase shift from −90° of the line standard between 8.2 and 12.4 GHz. The stepwise technique [23] was used for obtaining accurate m_b^+ and m_b^- branch indices by our method and by the methods [19,18]. Ten independent S-parameter measurements were conducted for our method and the methods [19,18] to examine standard deviations in the evaluation of propagation characteristics of this shifter.

Figs. 2 and 3 illustrate the determined T_1^+, T_1^-, γ_1^+, and γ_1^- quantities of the microwave phase shifter by our method using (16) and the methods [19,18] using average S-parameters of each individual ten measurement set. It is noted from Figs. 2 and 3 that determined T_1^+, T_1^-, γ_1^+, and γ_1^- of the microwave phase shifter by our proposed general LL method are in good agreement with those measured by the calibration-dependent method [19] and the calibration-independent method [18], thus validating the proposed formalism. It should here be noted that while the method [18] and our proposed method do not necessitate any formal calibration procedure, the method [19] requires such a procedure.

3.2. Accuracy analysis

In order to compare the accuracy of our proposed method in reference to the accuracy of the methods [19,18], we first examined the standard deviations of the extracted γ_1^+ and γ_1^-. For example, Fig. 4(a) demonstrates the standard deviations of α_1^+ at 10 GHz extracted by our method and by the methods [19,18]. Standard deviations of β_1^+, α_1^-, and β_1^- are not demonstrated for conciseness. It is observed from Fig. 4(a) that the standard deviation for α_1^+ at 10 GHz extracted by our method (comparable with that extracted by the calibration-dependent method [19]) is lower than that extracted by the calibration-independent method [18]. This indicates that our proposed method extracts fairly stable α_1^+ (β_1^+, α_1^-, and β_1^-), as compared with the calibration-independent method [18].

We then calculated the N-RMSE and GoF values for α_1^+, β_1^+, α_1^-, and β_1^- using the following expressions [25]

$$\chi_{\text{N-RMSE}} = \frac{\sqrt{\frac{1}{N_f}\left[\sum_{k=1}^{N_f}\left(\chi_k^{\rm ref} - \chi_k^{\rm ext}\right)^2\right]}}{\max(\chi^{\rm ext}) - \min(\chi^{\rm ext})}, \tag{18}$$

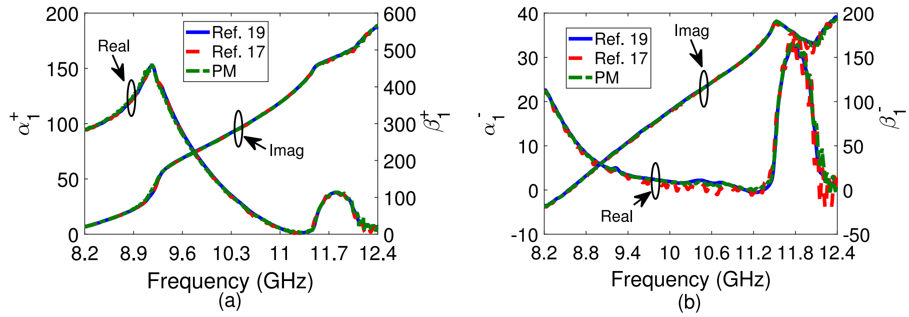

Fig. 3. Extracted (a) α_1^+ and β_1^+ and (b) α_1^- and β_1^- of the microwave phase shifter by the method in [19] (denoted by 19), the calibration-independent method [18] (denoted by Ref. [18]), and the proposed method (denoted by PM).

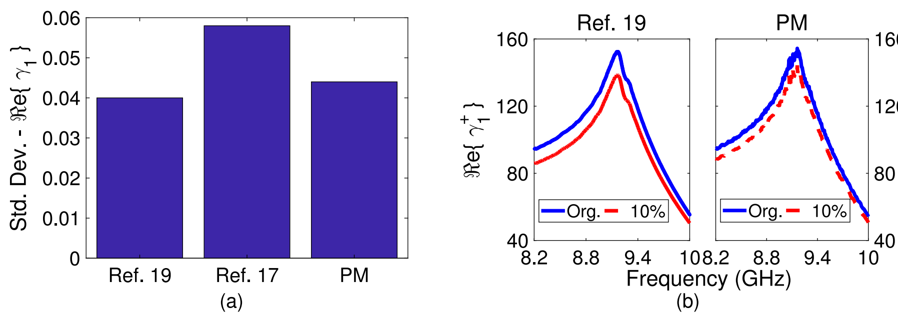

Fig. 4. (a) Calculated standard deviations of the real part of γ_1^+ and (b) extracted real part of γ_1^+ when $d = 28.7$ mm (denoted by 'Org.') and $d = 31.57$ mm (denoted by '10%' offset) of the microwave phase shifter by the method in [19] (denoted by Ref. [19]) and the proposed method (denoted by PM).

Table 1
Calculated $\alpha^+_{1,\text{N-RMSE}}$, $\alpha^-_{1,\text{N-RMSE}}$, $\beta^+_{1,\text{N-RMSE}}$, and $\beta^-_{1,\text{N-RMSE}}$ values using measured α_1^+, α_1^-, β_1^+, and β_1^- by our method and the method [18].

Method	$\alpha^+_{1,\text{N-RMSE}}$	$\alpha^-_{1,\text{N-RMSE}}$	$\beta^+_{1,\text{N-RMSE}}$	$\beta^-_{1,\text{N-RMSE}}$
[18]	0.0093	0.0228	0.0035	0.0098
Our method	0.0087	0.0211	0.0031	0.0085

Table 2
Calculated $\text{GoF}_{\alpha_1^+}$, $\text{GoF}_{\alpha_1^-}$, $\text{GoF}_{\beta_1^+}$, and $\text{GoF}_{\beta_1^-}$ values using measured α_1^+, α_1^-, β_1^+, and β_1^- by our method and the method [18].

Method	$\text{GoF}_{\alpha_1^+}$	$\text{GoF}_{\alpha_1^-}$	$\text{GoF}_{\beta_1^+}$	$\text{GoF}_{\beta_1^-}$
[18]	0.9706	0.8182	0.9885	0.9678
Our method	0.9750	0.9309	0.9004	0.9712

$$\text{GoF}_\chi = 1 - \frac{\left\|\chi^{\text{cal}} - \chi^{\text{ext}}\right\|^2}{\left\|\chi^{\text{cal}} - \chi^{\text{cal}}_{\text{mean}}\right\|^2}, \quad \chi^{\text{cal}}_{\text{mean}} = \frac{1}{N_f}\sum_{k=1}^{Nf}\chi_k^{\text{cal}}, \tag{19}$$

where χ stands for α_1^+, β_1^+, α_1^-, or β_1^-; χ_k^{ref} and χ_k^{ext} are the reference and extracted χ values at kth frequency point; N_f is the number of frequency points (for our case, $N_f = 1001$); $\|\cdot\|$ indicates the 2-norm of '$\cdot$'; and max($\star$) and min($\star$) are the maximum and minimum values of '$\star$', respectively. In our analysis, we consider the γ_1^+ and γ_1^- values extracted by the method [19] as the reference values to compare the accuracy of our method with the accuracy of the method [18]. It should be noted that the lower the $\alpha^+_{1,\text{N-RMSE}}$, $\alpha^-_{1,\text{N-RMSE}}$, $\beta^+_{1,\text{N-RMSE}}$, and $\beta^-_{1,\text{N-RMSE}}$ values are (or the higher the $\text{GoF}_{\alpha_1^+}$, $\text{GoF}_{\alpha_1^-}$, $\text{GoF}_{\beta_1^+}$, and $\text{GoF}_{\beta_1^-}$ values are), the better agreement the extracted and reference quantities have.

It is seen from Table 1 that calculated $\alpha^+_{1,\text{N-RMSE}}$, $\alpha^-_{1,\text{N-RMSE}}$, $\beta^+_{1,\text{N-RMSE}}$, and $\beta^-_{1,\text{N-RMSE}}$ values by our method are smaller than the corresponding calculated ones by the method [18]. Besides, it is also noted from Table 2 that calculated $\text{GoF}_{\alpha_1^+}$, $\text{GoF}_{\alpha_1^-}$, $\text{GoF}_{\beta_1^+}$, and $\text{GoF}_{\beta_1^-}$ values by our method are bigger than the corresponding calculated ones by the method [18]. These results clearly demonstrate that α_1^+, β_1^+, α_1^-, or β_1^- values extracted by our method are, respectively, closer to the reference values determined by the method [19] than those extracted by the method [18].

Aside from the accuracy analysis based on N-RMSE and GoF values for the extracted α_1^+, β_1^+, α_1^-, or β_1^- parameters by our method, we additionally performed a statistical analysis involving COV and CI to quantitatively examine the confidence level of extracted α_1^+, β_1^+, α_1^-, or β_1^- parameters by our method. COV and CI values can be determined from the following expressions [26]

$$\chi_{av} = \frac{1}{N_f}\sum_{k=1}^{N_f}\chi_k, \quad \sigma_\chi = \sqrt{\frac{1}{N_f}\sum_{k=1}^{N_f}(\chi_k - \chi_{av})^2}, \tag{20}$$

$$\text{COV}_\chi = \frac{\sigma_\chi}{\chi_{av}}, \quad \text{CI}_\chi = t\frac{\text{COV}_\chi}{\sqrt{N_s}}\chi_{av}, \quad \chi_k - \text{CI}_\chi < \chi_k^{\text{ref}} < \chi_k + \text{CI}_\chi. \tag{21}$$

Here, χ_{av} and σ_χ are, respectively, the average and standard deviations of χ; COV_χ and CI_χ are, respectively, the COV and CI values of χ; N_s corresponds to the number independent measurement carried out (for our case, $N_s = 10$); and t is the quantity corresponding to the selected CI value in the t-distribution table. The quantities χ_k^{ref} and N_f are presented before. t values corresponding to CI values of 90% and 95% are evaluated as 1.833 and 2.262, respectively. In our analysis, we also consider the γ_1^+ and γ_1^- values extracted by the method [19] as the reference values.

Table 3 illustrates calculated COV values and CI ranges for the $\alpha^+_{1,k}$, $\beta^+_{1,k}$, $\alpha^-_{1,k}$, or $\beta^-_{1,k}$ parameters extracted by our method at the frequency 10.3 GHz (at the mid frequency of the X-band). It is observed from 3 that the $\alpha^+_{1,av}$, $\alpha^-_{1,av}$, $\beta^+_{1,av}$, and $\beta^-_{1,av}$ values evaluated from the extracted parameters by our method lie within the 90% CI range (also the 90% CI range). Besides, it is noted from Table 3 that $\Delta\alpha^+_{1,av}/\alpha^{+\text{ref}}_{1,k} < \Delta\alpha^-_{1,av}/\alpha_k^{-\text{ref}}$ and $\Delta\beta^+_{av}/\beta_k^{+\text{ref}} < \Delta\beta^-_{av}/\beta_k^{-\text{ref}}$, which can be due to the point that α_1^- and β_1^- are evaluated after finding α_1^+ and β_1^+ in application of our method. To evaluate whether α_1^+, α_1^-, β_1^+, and β_1^- values lie within 90% CI range over whole frequency band, we calculated $\alpha^+_{1,k}$, $\beta^+_{1,k}$, $\alpha^-_{1,k}$, or $\beta^-_{1,k}$

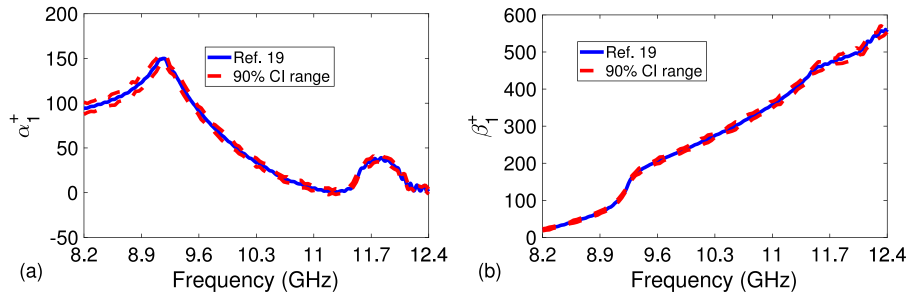

Fig. 5. Extracted (a) α_1^+ and (b) β_1^+ by the method [19] and by our method for 90% CI range.

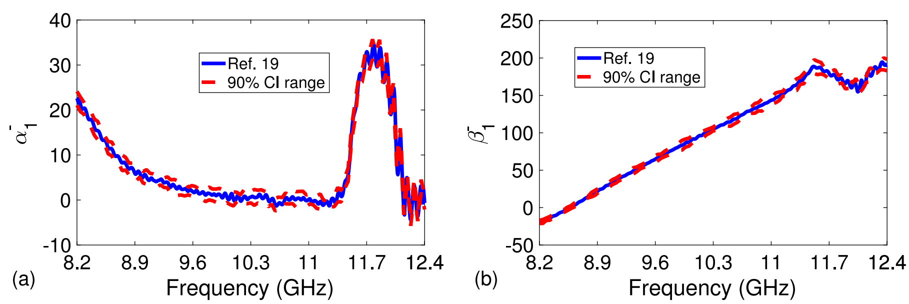

Fig. 6. Extracted (a) α_1^- and (b) β_1^- by the method [19] and by our method for 90% CI range.

Table 3
Calculated COV values and CI ranges for the α_1^+, β_1^+, α_1^-, or β_1^- parameters extracted by our method at the frequency 10.3 GHz.

$\alpha_{1,k}^{+\ \mathrm{ref}}$	$\alpha_{1,av}^+$	$\Delta\alpha_{1,av}^+/\alpha_{1,k}^{+\ \mathrm{ref}}$	COV	CI (90%) range	CI (95%) range
33.3220	34.1345	2.44%	0.0649	32.37–34.90	32.07–35.20
$\alpha_{1,k}^{-\ \mathrm{ref}}$	$\alpha_{1,av}^-$	$\Delta\alpha_{1,av}^-/\alpha_{1,k}^{-\ \mathrm{ref}}$	COV	CI (90%) range	CI (95%) range
0.6232	0.6011	3.55%	0.0845	0.596–0.658	0.589–0.665
$\beta_{1,k}^{+\ \mathrm{ref}}$	$\beta_{1,av}^+$	$\Delta\beta_{1,av}^+/\beta_{1,k}^{+\ \mathrm{ref}}$	COV	CI (90%) range	CI (95%) range
275.68	273.149	0.92%	0.0138	272.5–277.0	272.0–277.5
$\beta_{1,k}^{-\ \mathrm{ref}}$	$\beta_{1,av}^-$	$\Delta\beta_{1,av}^-/\beta_{1,k}^{-\ \mathrm{ref}}$	COV	CI (90%) range	CI (95%) range
105.62	104.15	1.39%	0.0256	103.7–106.8	103.3–107.2

values for each individual frequency over entire X-band. Figs. 5 and 6 demonstrate the dependencies of α_1^+, α_1^-, β_1^+, and β_1^- extracted by our method for the 90% CI range, in reference to the values extracted by the method [19]. It is observed from Figs. 5 and 6 that α_1^+, α_1^-, β_1^+, and β_1^- values extracted by our method are in good agreement for the 90% CI range, in reference to the α_1^+, α_1^-, β_1^+, and β_1^- values extracted by the method [19].

On the other hand, Fig. 4(b) shows the effect of inaccurate knowledge of l_1 on extracted α_1^+ for our method and the method [19]. Extracted β_1^+, α_1^-, and β_1^- are not demonstrated for simplicity. It is seen from 4(b) that our proposed method is less affected by 10% offset from the actual value of $l_1 = 28.7$ mm than the method [19]. These results indicate that our method not only extracts more accurate γ_1^+ (and γ_1^-) but also alleviates the effect of inaccurate information of l_1 on extracted γ_1^+ (and γ_1^-) through using multiple reference lines. Finally, it is noted that in application of our methodology, we did not consider the effect of switching errors in extracting γ_1^+ and γ_1^- values [27,28]. Although the procedure used to eliminating switching errors [25] barely improves the accuracy of our method for the VNA used in our measurements, it may be largely effective especially for some VNAs with improper forward and/or backward impedance termination at the VNA source.

4. Conclusion

A generalized LL method is proposed for propagation constant measurement of nonreciprocal networks. Its formalism considers a reference network having arbitrary forward and backward propagation constants, impedance, and length. The method is useful especially for improving the measurement accuracy and reducing the effect of inaccurate length information of the non-reciprocal line/network. Analyses based on N-RMSE and GoF values and based on COV and CI values show that the accuracy of our generalized line-line method for propagation constant measurement of nonreciprocal networks is better than the accuracy of other line-line method utilized for the same goal in the literature.

CRediT authorship contribution statement

Ugur Cem Hasar: Conceptualization, Methodology, Investigation, Writing – original draft. **Hamdullah Ozturk:** Visualization, Writing – review & editing. **Huseyin Korkmaz:** Visualization, Writing – review & editing. **Mucahit Izginli:** Visualization, Writing – review & editing. **Muharrem Karaaslan:** Investigation, Writing – review & editing. **Musa Bute:** Investigation, Writing – review & editing.

Declaration of competing interest

The authors declare that they have no known competing financial interests or personal relationships that could have appeared to influence the work reported in this paper.

Data availability

The data that has been used is confidential.

Acknowledgments

Authors would like to thank the Scientific and Technological Research Council of Turkey (TUBITAK) under the project number 120M763 for supporting this study. Besides, the authors, H. Ozturk and H. Korkmaz, acknowledge the TUBITAK BIDEB 2211/C program for supporting their studies.

References

[1] Z. Caijun, J. Quanxing, J. Shenhui, Calibration-independent and position-insensitive transmission/reflection method for permittivity measurement with one sample in coaxial line, IEEE Trans. Electromagn. Compat. 53 (3) (2011) 684–689.

[2] M.Q. Lee, S. Nam, An accurate broadband measurement of substrate dielectric constant, IEEE Microw. Guid. Wave Lett. 6 (4) (1996) 168–170.

[3] I. Huygen, C. Steukers, F. Duhamel, A wideband line-line dielectrometric method for liquids, soils, and planar substrates, IEEE Trans. Instrum. Meas. 50 (5) (2001) 1343–1348.

[4] C. Wan, B. Nauwelaers, W.D. Raedt, M.V. Rossum, Two new measurement methods for explicit determination of complex permittivity, IEEE Trans. Microw. Theory Tech. 46 (11) (1998) 1614–1619.

[5] K. Grenier, D. Dubuc, P. Poleni, M. Kumemura, H. Toshiyoshi, T. Fujii, H. Fujita, Integrated broadband microwave and microfluidic sensor dedicated to bioengineering, IEEE Trans. Microw. Theory Tech. 57 (12) (2009) 3246–3253.

[6] M.D. Janezic, J.A. Jargon, Complex permittivity determination from propagation constant measurements, IEEE Microw. Guid. Wave Lett. 9 (2) (1999) 76–78.

[7] L. Lanzi, M. Carla, C.M.C. Gambi, L. Lanzi, Differential and double-differential dielectric spectroscopy to measure complex permittivity in transmission lines, Rev. Sci. Instrum. 73 (8) (2002) 3085–3088.

[8] C. Wan, B. Nauwelaers, W.D. Raedt, M.V. Rossum, Complex permittivity measurement method based on asymmetry of reciprocal two-ports, Electron. Lett. 32 (16) (1996) 1497.

[9] U.C. Hasar, O.E. Inan, A position-invariant calibration-independent method for permittivity measurement, Microw. Opt. Technol. Lett. 51 (6) (2009) 1406–1408.

[10] N.J. Farcich, J. Salonen, P.M. Asbeck, Single-length method used to determine the dielectric constant of polydimethylsiloxane, IEEE Trans. Microw. Theory Tech. 56 (12) (2008) 2963–2971.

[11] U.C. Hasar, A new calibration-independent method for complex permittivity extraction of solid dielectric materials, IEEE Microw. Wirel. Compon. Lett. 18 (12) (2008) 788–790.

[12] U.C. Hasar, Calibration-independent method for complex permittivity determination of liquid and granular materials, Electron. Lett. 44 (9) (2008) 585–586.

[13] U.C. Hasar, A calibration-independent method for accurate complex permittivity determination of liquid materials, Rev. Sci. Instrum. 79 (8) (2008) 086114.

[14] N. Jebbor, S. Bri, A.M. Sànchez, M. Chaibi, A fast calibration-independent method for complex permittivity determination at microwave frequencies, Measurement 46 (7) (2013) 2206–2209.

[15] C. Guoxin, Calibration-independent measurement of complex permittivity of liquids using a coaxial transmission line, Rev. Sci. Instrum. 86 (1) (2015) 014704.

[16] U.C. Hasar, H. Ozturk, H. Korkmaz, M. Izginli, M. Karaaslan, Improved line–line method for propagation constant measurement of reflection-asymmetric networks, Measurement 192 (2022) 110848.

[17] U.C. Hasar, Y. Kaya, M. Ertugrul, Measurement of propagation characteristics of nonreciprocal networks/lines using a line-line method, IEEE Trans. Electromagn. Compat. 63 (4) (2021) 1240–1247.

[18] U.C. Hasar, Y. Kaya, G. Ozturk, M. Ertugrul, Propagation constant measurements of reflection-asymmetric and nonreciprocal microwave networks from S-parameters without using a reflective standard, Measurement 165 (2020) 108126.

[19] R. Zhao, T. Koschny, C.M. Soukoulis, Chiral metamaterials: Retrieval of the effective parameters with and without substrate, Opt. Express 18 (14) (2010) 14553—14567.

[20] U.C. Hasar, M. Bute, Method for retrieval of electromagnetic properties of inhomogeneous reciprocal chiral metamaterials, IEEE Trans. Antennas Propag. 68 (7) (2020) 5714–5717.

[21] R.B. Marks, A multiline method of network analyzer calibration, IEEE Trans. Microw. Theory Tech. 39 (7) (1991) 1205–1215.

[22] J.A. Reynoso-Hernandez, Unified method for determining the complex propagation constant of reflecting and nonreflecting transmission lines, IEEE Microw. Wirel. Compon. Lett. 13 (8) (2003) 351–353.

[23] U.C. Hasar, J.J. Barroso, C. Sabah, Y. Kaya, M. Ertugrul, Stepwise technique for accurate and unique retrieval of electromagnetic properties of bianisotropic metamaterials, J. Opt. Soc. Amer. B 30 (4) (2013) 1058–1068.

[24] J.J. Barroso, U.C. Hasar, Constitutive parameters of a metamaterial slab retrieved by the phase unwrapping method, J. Infrared Millim. Terahz Waves 33 (2012) 237–244.

[25] U.C. Hasar, T. Ince, M. Bute, Application of the singular spectrum analysis technique for phase constant determination of symmetric reflecting and nonreflecting lines, IEEE Trans. Electromagn. Compat. 62 (2) (2020) 571–579.

[26] U.C. Hasar, Y. Kaya, G. Ozturk, M. Ertugrul, Effect of sample deformation in longitudinal axis on material parameter extraction by waveguides, Measurement 176 (2021) 109175.

[27] R.B. Marks, Formulations of the basic vector network analyzer error model including switch terms, in: Proc. 50th ARFTG Conf. Dig, 1997, pp. 115—126.

[28] D.C. DeGroot, J.A. Jargon, R.B. Marks, Multiline TRL revealed, in: 60th ARFTG Conference Digest, 2002, pp. 131–155.